VOL. 16, NO. 14, JULY 2021 ISSN 1819-6608
ARPN Journal of Engineering and Applied Sciences
©2006-2021 Asian Research Publishing Network (ARPN). All rights reserved.
www.arpnjournals.com

# SPATIAL DISTRIBUTED CONTROL SYSTEM OF TEMPERATURE FIELD: SYNTHESIS AND MODELING

Yury Ilyushin and Olga Afanaseva
Saint-Petersburg Mining University, Vasilyevsky Island, 21st line, Saint-Petersburg, Russia
E-Mail: ilyushin_y@bk.ru, Ovaf72@gmail.com

## ABSTRACT

In modern conditions, glass and glass products are becoming more and more demanded in various industries. At the same time, the industry makes more and more stringent requirements for the quality of products. This requirement forces glass manufacturers to improve production technologies aimed at improving the quality and reducing the cost of production. This research work is devoted to the sheet stack production technology modernization through the development and implementation of a high-precision distributed controller. The paper analyzes the existing system, synthesizes a regulator and performs mathematical modeling of the resulting system. This work can be useful both for the manufacturer of the sheet stack, and for specialists in the field of mathematical and computer modeling.

**Keywords:** analysis, synthesis, control, temperature field, modeling.

## INTRODUCTION

Glass production is based on the use of natural ingredients, which do not lose their quality during recycling and do not leave waste. Glass has several options for its aggregation state at different stages of production. It is an amorphous body consisting of soda, silica sand, dolomite, limestone and various additives. It is obtained by the melt method and in the solid state it loses the properties of a crystalline substance. Glass production is a complex technological process based on knowledge of chemical formulas and requires a lot of investment. The classical method is based on the smelting of raw materials with the addition of amplifiers, dyes, mufflers and decolourizers. The resulting mass is cooled so that there are no small crystals. It should unite into a monolith. Today, flat glass is the main product of the industry. Glass making technology is based on the use of special equipment broken down into a number of stages [2].

At the first technological stage of raw material preparation, along with simple installations, high-tech units are used. The ingredients are transported by conveyors. Cleaning of harmful impurities is carried out by sophisticated machines, among which there are magnetic separators. They extract metals from sand that can spoil the properties of the finished product. To grind the substance, powerful crushers are used.

The second stage of production is associated with the preparation of the charge. The choice of components depends on the finished product properties. In this case, special equipment is used. High-precision scales help to calculate the correct dosage. With their help, the required amount of quartz sand, soda, lime is measured. If necessary, minor materials that determine the strength, color, light transmittance of the glass product are added. The prepared components are fed into the batch mixer, which evenly distributes the materials throughout the mass.

The third, main stage, involves glass melting in special furnaces with individual thermal and technological modes. Glass furnace equipment differs both in the principle of heating and in the method of forming the thermal field. Flame stoves are designed to burn fuel. They have a low coefficient of efficiency since heat energy is distributed to heating the charge and boilers. Electrical equipment allows the production of any type of glass. They need current to power them. Glass melt is used as a heater - it is it that acts as an electrolyte at high temperatures. During the operation of electric furnaces, there is no heat loss with waste gases. Combined gas-electric plants combine two types of thermal energy sources. The combustion of gas heats up and melts the charge; the molten glass acquires a high temperature by direct resistance.

At the fourth and final stage of glass production, the final product is formed.

The work is devoted to the analysis of the third stage of production and the issuance of recommendations for improving the production technology in order to reduce the cost of the final product and increase in quality.

## FORMULATION OF THE PROBLEM

Glass defects are various particles or gas bubbles that get inside the glass during its processing. If we consider all defects as a whole, then most of them fall on defects associated with a poor-quality edge of the product and with incorrect temperature treatment of the product. The appearance of the product is lost. To correct the defect, depending on the manufacturing method of this product, it is reheated. In principle, the appearance of the edge can also be adjusted through the peephole by adjusting the temperature and phases, but it is extremely inaccurate. If after all the manipulations with the aging phases, the languor did not lead to a positive result and the edge still remains, or the rough or burnt edge is polished [1].

Another common thermal defect is the appearance of a tear - the so-called trail formed when glass adheres to a substrate or glass mold. With this defect, the main method of struggle is the high-quality preparation of glass molds for use, prevention of burnout of the glaze itself and complete removal of moisture from the surfaces

©2006-2021 Asian Research Publishing Network (ARPN). All rights reserved.


of molds and substrates, as well as exceptional control of the product heat treatment.

The appearance of bubbles, that is, air-filled cavities located between the layers of glass, is also associated with poor-quality heat treatment of the product. You can also find it in products. To get rid of them, it is recommended to provide a slow high-precision heating of products to a temperature of 600-700 degrees. In this case, the air will leave naturally.

The production of ceramic products consists of the raw materials processing and mass preparation, the formation of products, drying, firing and decoration. The processing of raw materials and the preparation of ceramic mass are reduced to cleaning the raw material from extraneous (mainly coloring) impurities, coarse and fine grinding, mixing in accordance with the recipe, thorough mixing and vacuuming of the mass. Impurities of titanium and iron oxides cause yellowish, grayish shades of the shard, and the heterogeneity of the mass is the cause of the deformations, cracks, irregularities.

Ceramic production is based on the characteristic properties of clay materials - the ability to form plastic dough with water and easily form, maintain cohesion in a dry state and acquire strength and hardness after firing. Clay materials, especially kaolin, increase the whiteness, strength, chemical and thermal stability of fired products. Materials for decorating ceramics are ceramic paints, preparations of precious metals, chandeliers. Ceramic paints are subdivided into overglaze, intraglaze and underglaze paints.

Thus, the processes for the glass and ceramic products production are similar to each other. This is due to both the identity of the furnaces used for the material temperature treatment and the identity of the heat treatment process course. In order to improve the quality of manufactured products, let us consider the problem of a temperature field control system analysis and synthesis for the sheet furnace for pouring glass and ceramics.

## METHODOLOGY

Casting production process consists of several stages: 1. Raw material preparation process; glass melting process; molding and cooling of molten glass; the process of heat treatment (tempering) of glass.

Consider the glass tempering process in a special chamber design.

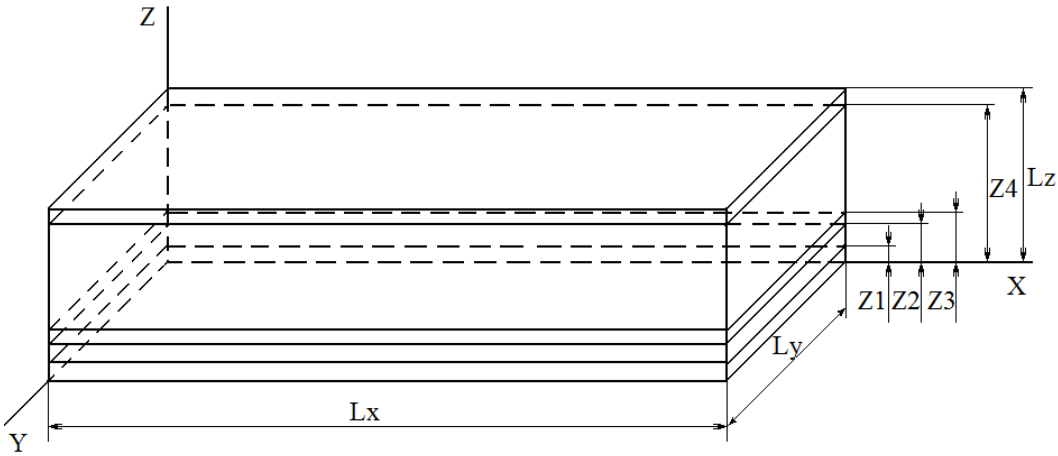


**Figure-1.** The main dimensions of the heating chamber for heat treatment of glass.

Taking into account Figure-1 the mathematical model of the heating chamber thermal processes can be written in the form [7, 10]:

$$\frac{\partial T}{\partial \tau} = a1 \cdot \left( \frac{\partial^2 T}{\partial x^2} + \frac{\partial^2 T}{\partial y^2} + \frac{\partial^2 T}{\partial y^2} \right), \; T = T(X, Y, Z, \tau) \quad (1)$$

$$0 < X < Lx, \; 0 < Y < Ly, \; 0 < Z < Z1, \; \tau > 0,$$

$$\frac{\partial T}{\partial \tau} = a2 \cdot \left( \frac{\partial^2 T}{\partial x^2} + \frac{\partial^2 T}{\partial y^2} + \frac{\partial^2 T}{\partial y^2} \right), \; T = T(X, Y, Z, \tau) \quad (2)$$

$$0 < X < Lx, \; 0 < Y < Ly, \; Z1 < Z < Z2, \; \tau > 0,$$

$$\frac{\partial T}{\partial \tau} = a3 \cdot \left( \frac{\partial^2 T}{\partial x^2} + \frac{\partial^2 T}{\partial y^2} + \frac{\partial^2 T}{\partial y^2} \right), \; T = T(X, Y, Z, \tau) \quad (3)$$

$$0 < X < Lx, \; 0 < Y < Ly, \; Z2 < Z < Z3, \; \tau > 0,$$

$$\frac{\partial T}{\partial \tau} = a4 \cdot \left( \frac{\partial^2 T}{\partial x^2} + \frac{\partial^2 T}{\partial y^2} + \frac{\partial^2 T}{\partial y^2} \right), \; T = T(X, Y, Z, \tau) \quad (4)$$

$$0 < X < Lx, \; 0 < Y < Ly, \; Z3 < Z < Z4, \; \tau > 0,$$

$$\frac{\partial T}{\partial \tau} = a5 \cdot \left( \frac{\partial^2 T}{\partial x^2} + \frac{\partial^2 T}{\partial y^2} + \frac{\partial^2 T}{\partial y^2} \right), \; T = T(X, Y, Z, \tau) \quad (5)$$

$$0 < X < Lx, \; 0 < Y < Ly, \; Z4 < Z < Lz, \; \tau > 0,$$

©2006-2021 Asian Research Publishing Network (ARPN). All rights reserved.


where a1, a2, a3, a4, a5 - thermal diffusivity coefficients, *X*, *Y*, *Z* - spatial coordinates, τ - time.

Boundary conditions under which the obtained system of differential equations (1-5) should be solved and are written with taking into account the following assumption: we will assume that the heating chamber is completely insulated with the exception of two side surfaces. In this case, the boundary conditions will have the form [6, 13, 14]:

$$\frac{\partial T(X,0,Z,\tau)}{\partial y}=0, \quad (6)$$

$$\frac{\partial T(X,Ly,Z,\tau)}{\partial y}=0, \text{ where } 0\le X\le Lx,\ 0\le Z\le Lz, \quad (7)$$

$$\frac{\partial T(X,Y,0,\tau)}{\partial z}=0, \quad (8)$$

$$\frac{\partial T(X,Y,Lz,\tau)}{\partial z}=0, \text{ where } 0\le X\le Lx,\ 0\le Y\le Ly, \quad (9)$$

$$T(0,Y,Z,\tau)=const, \quad (10)$$

$$T(Lx,Y,z,\tau)=const, \text{ where } 0\le Z\le Lz,\ 0\le Y\le Ly. \quad (11)$$

Next, we write down the conditions at the interfaces:

$$\lambda 1\cdot\frac{\partial T(X,Y,Z1,\tau)}{\partial z}=\lambda 2\cdot\frac{\partial T(X,Y,Z1,\tau)}{\partial z}, \text{ where } 0\le X\le Lx,\ 0\le Z\le Lz, \quad (12)$$

$$\lambda 2\cdot\frac{\partial T(X,Y,Z2,\tau)}{\partial z}=\lambda 3\cdot\frac{\partial T(X,Y,Z2,\tau)}{\partial z}, \text{ where } 0\le X\le Lx,\ 0\le Z\le Lz, \quad (13)$$

$$\lambda 3\cdot\frac{\partial T(X,Y,Z3,\tau)}{\partial z}=\lambda 4\cdot\frac{\partial T(X,Y,Z3,\tau)}{\partial z}, \text{ where } 0\le X\le Lx,\ 0\le Z\le Lz, \quad (14)$$

$$\lambda 4\cdot\frac{\partial T(X,Y,Z4,\tau)}{\partial z}=\lambda 5\cdot\frac{\partial T(X,Y,Z4,\tau)}{\partial z}, \text{ where } 0\le X\le Lx,\ 0\le Z\le Lz. \quad (15)$$

When solving the system of differential equations (1-5) taking into account the boundary conditions (6-15), the initial conditions are assumed to be zero.

Further, the resulting system of equations, for solving it on a computer, is converted into a discrete form. To discretize the heating chamber for glass heat treatment, we will replace the variables X, Y, Z, τ with their discrete integer analogs x, y, z, μ. Then a discrete mathematical model of thermal processes of the heating chamber can be written in the form [10, 12, 4, 5]:

$$\frac{T_{x,y,z,\mu}-T_{x,y,z,\mu-1}}{\partial\tau}=a1\cdot\left(\frac{T_{x+1,y,z,\mu-1}-2\cdot T_{x,y,z,\mu-1}+T_{x-1,y,z,\mu-1}}{\partial x^2}+\right.$$
$$\left.+\frac{T_{x,y+1,z,\mu-1}-2\cdot T_{x,y,z,\mu-1}+T_{x,y-1,z,\mu-1}}{\partial y^2}+\frac{T_{x,y,z+1,\mu-1}-2\cdot T_{x,y,z,\mu-1}+T_{x,y,z-1,\mu-1}}{\partial z^2}\right), \quad (16)$$
$$0<x<NLx,\ 0<y<NLy,\ 0<z<NZ1,\ \mu>0.$$

$$\frac{T_{x,y,z,\mu}-T_{x,y,z,\mu-1}}{\partial\tau}=a2\cdot\left(\frac{T_{x+1,y,z,\mu-1}-2\cdot T_{x,y,z,\mu-1}+T_{x-1,y,z,\mu-1}}{\partial x^2}+\right.$$
$$\left.+\frac{T_{x,y+1,z,\mu-1}-2\cdot T_{x,y,z,\mu-1}+T_{x,y-1,z,\mu-1}}{\partial y^2}+\frac{T_{x,y,z+1,\mu-1}-2\cdot T_{x,y,z,\mu-1}+T_{x,y,z-1,\mu-1}}{\partial z^2}\right), \quad (17)$$
$$0<x<NLx,\ 0<y<NLy,\ NZ1<z<NZ2,\ \mu>0.$$

$$\frac{T_{x,y,z,\mu}-T_{x,y,z,\mu-1}}{\partial\tau}=a3\cdot\left(\frac{T_{x+1,y,z,\mu-1}-2\cdot T_{x,y,z,\mu-1}+T_{x-1,y,z,\mu-1}}{\partial x^2}+\right.$$
$$\left.+\frac{T_{x,y+1,z,\mu-1}-2\cdot T_{x,y,z,\mu-1}+T_{x,y-1,z,\mu-1}}{\partial y^2}+\frac{T_{x,y,z+1,\mu-1}-2\cdot T_{x,y,z,\mu-1}+T_{x,y,z-1,\mu-1}}{\partial z^2}\right), \quad (18)$$
$$0<x<NLx,\ 0<y<NLy,\ NZ2<z<NZ3,\ \mu>0.$$

©2006-2021 Asian Research Publishing Network (ARPN). All rights reserved.


$$\frac{T_{x,y,z,\mu}-T_{x,y,z,\mu-1}}{\partial\tau}=a4\cdot\left(\frac{T_{x+1,y,z,\mu-1}-2\cdot T_{x,y,z,\mu-1}+T_{x-1,y,z,\mu-1}}{\partial x^2}+\right.$$
$$\left.+\frac{T_{x,y+1,z,\mu-1}-2\cdot T_{x,y,z,\mu-1}+T_{x,y-1,z,\mu-1}}{\partial y^2}+\frac{T_{x,y,z+1,\mu-1}-2\cdot T_{x,y,z,\mu-1}+T_{x,y,z-1,\mu-1}}{\partial z^2}\right), \quad (19)$$
$0<x<NLx$, $0<y<NLy$, $NZ3<z<NZ4$, $\mu>0$.

$$\frac{T_{x,y,z,\mu}-T_{x,y,z,\mu-1}}{\partial\tau}=a5\cdot\left(\frac{T_{x+1,y,z,\mu-1}-2\cdot T_{x,y,z,\mu-1}+T_{x-1,y,z,\mu-1}}{\partial x^2}+\right.$$
$$\left.+\frac{T_{x,y+1,z,\mu-1}-2\cdot T_{x,y,z,\mu-1}+T_{x,y-1,z,\mu-1}}{\partial y^2}+\frac{T_{x,y,z+1,\mu-1}-2\cdot T_{x,y,z,\mu-1}+T_{x,y,z-1,\mu-1}}{\partial z^2}\right), \quad (20)$$
$0<x<NLx$, $0<y<NLy$, $NZ4<z<NLz$, $\mu>0$.

In discrete form, the boundary conditions will have the form: $\frac{\partial T(x,0,z,\mu)}{\partial y}=0$, from where

$$T(x,0,z,\mu)=T(x,1,z,\mu),\ \frac{\partial T(x,NLy,x,\mu)}{\partial y}=0, \quad (21)$$

then

$T(x,NLy,x,\mu)=T(x,NLy-1,x,\mu)$, where
$0\le x\le NLx$, $0\le z\le NLz$, $\mu\ge 0$. (22)

$$\frac{\partial T(x,y,0,\mu)}{\partial z}=0,$$

from where

$$T(x,y,0,\mu)=T(x,y,1,\mu),\ \frac{\partial T(x,y,NLz,\mu)}{\partial z}=0 \quad (23)$$

and

$T(x,y,NLz,\mu)=T(x,y,NLz-1,\mu)$, where
$0\le x\le NLx$, $0\le y\le NLy$, $\mu\ge 0$. (24)

$$T(0,y,z,\mu)=const, \quad (25)$$

$T(NLx,y,z,\tau)=const$, where
$0\le z\le NLz$, $0\le y\le NLy$, $\mu\ge 0$. (26)

Next, we write down the conditions at the interfaces: $\lambda1\cdot\frac{\partial T(x,y,NZ1,\mu)}{\partial z}=\lambda2\cdot\frac{\partial T(x,y,NZ1)}{\partial z}$.

We get that

$$\lambda1\cdot\frac{T(x,y,NZ1-1,\mu)-T(x,y,NZ1,\mu)}{\partial z}=\lambda2\cdot\frac{T(x,y,NZ1)-T(x,y,NZ1+1,\mu)}{\partial z},$$

$$T(x,y,NZ1,\mu)=\frac{\lambda1\cdot T(x,y,NZ1-1,\mu)+\lambda2\cdot T(x,y,NZ1+1,\mu)}{\lambda1+\lambda2}, \quad (27)$$

where $0\le x\le NLx$, $0\le z\le NLz$, $\mu\ge 0$.

$$\lambda2\cdot\frac{\partial T(x,y,NZ2,\mu)}{\partial z}=\lambda3\cdot\frac{\partial T(x,y,NZ2)}{\partial z},$$

from where

$$\lambda2\cdot\frac{T(x,y,NZ2-1,\mu)-T(x,y,NZ2,\mu)}{\partial z}=\lambda3\cdot\frac{T(x,y,NZ2)-T(x,y,NZ2+1,\mu)}{\partial z},$$

$$T(x,y,NZ2,\mu)=\frac{\lambda2\cdot T(x,y,NZ2-1,\mu)+\lambda3\cdot T(x,y,NZ2+1,\mu)}{\lambda2+\lambda3}$$

, where $0\le x\le NLx$, $0\le z\le NLz$, $\mu\ge 0$. (28)

$$\lambda3\cdot\frac{\partial T(x,y,NZ3,\mu)}{\partial z}=\lambda4\cdot\frac{\partial T(x,y,NZ3)}{\partial z},$$

then

$$\lambda3\cdot\frac{T(x,y,NZ3-1,\mu)-T(x,y,NZ3,\mu)}{\partial z}=\lambda4\cdot\frac{T(x,y,NZ3)-T(x,y,NZ3+1,\mu)}{\partial z};$$

$$T(x,y,NZ3,\mu)=\frac{\lambda3\cdot T(x,y,NZ3-1,\mu)+\lambda4\cdot T(x,y,NZ3+1,\mu)}{\lambda3+\lambda4}$$

, where $0\le x\le NLx$, $0\le z\le NLz$, $\mu\ge 0$; (29)

$$\lambda4\cdot\frac{\partial T(x,y,NZ4,\mu)}{\partial z}=\lambda5\cdot\frac{\partial T(x,y,NZ4)}{\partial z},$$

consequently

$$\lambda4\cdot\frac{T(x,y,NZ4-1,\mu)-T(x,y,NZ4,\mu)}{\partial z}=\lambda5\cdot\frac{T(x,y,NZ4)-T(x,y,NZ4+1,\mu)}{\partial z};$$

$$T(x,y,NZ4,\mu)=\frac{\lambda4\cdot T(x,y,NZ4-1,\mu)+\lambda5\cdot T(x,y,NZ4+1,\mu)}{\lambda4+\lambda5},$$

where $0\le x\le NLx$, $0\le z\le NLz$, $\mu\ge 0$. (30)

The thermal diffusivity coefficient a of substances is determined from the following relation [7, 10, 11]:

©2006-2021 Asian Research Publishing Network (ARPN). All rights reserved.


$$a = \frac{\lambda}{c \cdot \gamma}, \left[\frac{m^2}{s}\right],$$

where $\gamma\left[\frac{kg}{m^3}\right]$ - density, $\lambda\left[\frac{W}{m * \text{degree}}\right]$ - thermal conductivity coefficient, $c\left[\frac{J}{kg * \text{degree}}\right]$ - heat capacity coefficient.

## ANALYSIS OF THE CONTROL OBJECT

As a result of the partial differential equations system numerical solution in each of the media, the following graphs of transient processes were obtained:

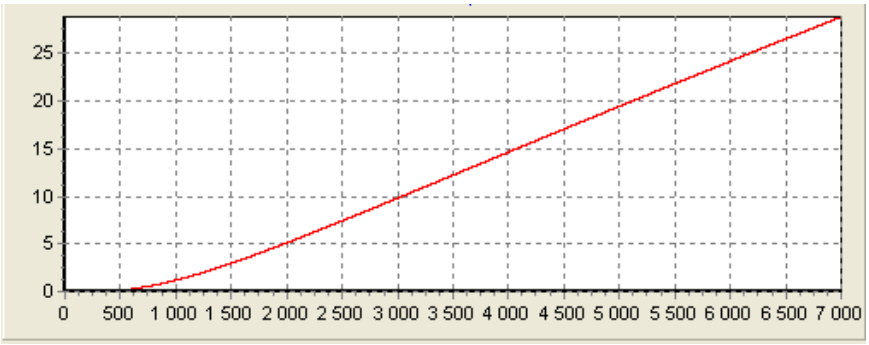


**Figure-2.** Graph of the transient process in the lead environment.

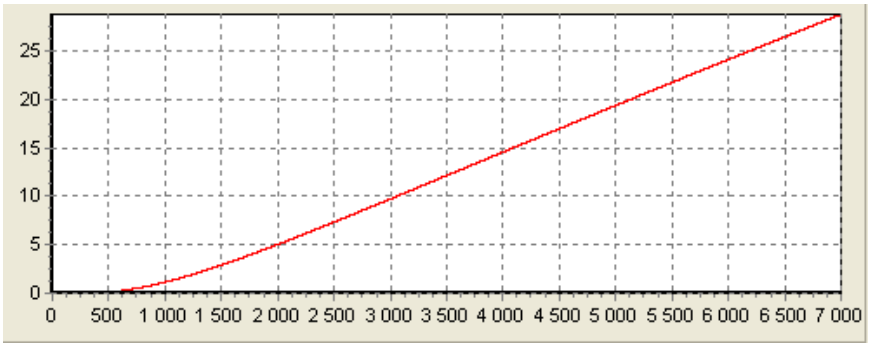


**Figure-3.** Graph of the transient in the environment of steel.

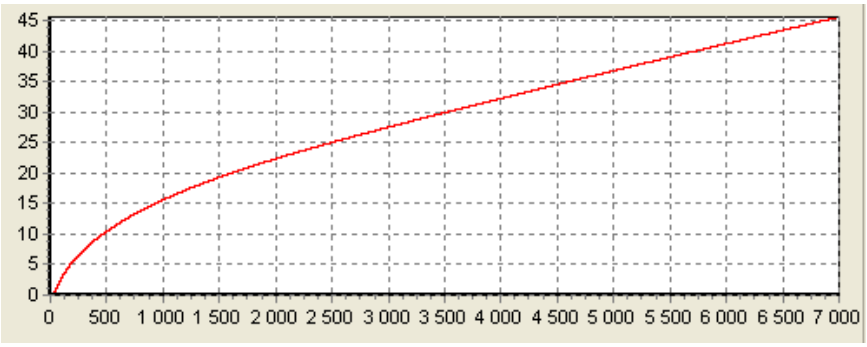


**Figure-4.** Graph of transient in glass environment.

©2006-2021 Asian Research Publishing Network (ARPN). All rights reserved.


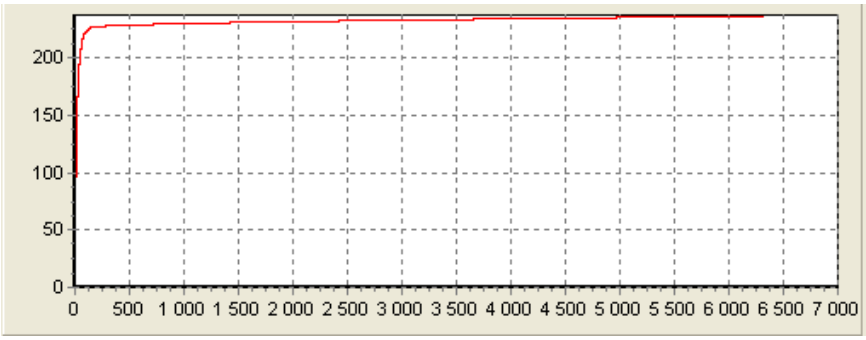


**Figure-5.** Transient graph in air.

As the results of the mathematical model calculations show, the computational scheme is stable, and the graphs of transient processes reflect real physical facts. Next, we proceed to the analysis of the control object in order to build a control system for it.

To analyze the control object, it is necessary to determine the function of the distributed input action on this object [3, 4, 5, 8].

Taking into account the fact that two sides of the heating chamber are thermally insulated, and two have a constant temperature, the input action on this object will be expanded in a series using the function *sin(Θ)* and *cos(Θ)*. In this case, the input action on the distributed object can be represented as:

$$T(x,y)=\sum_{i=1}^{N}\sum_{j=1}^{M}A(\tau)+B_{ij}\cdot\sin(\psi_i\cdot x)\cdot\cos(\chi_j\cdot y),$$

$$0<x<Lx,\ 0<y<Ly,\ \tau>0,$$

$$\psi_i=\frac{2\pi\cdot i}{Lx},\ (i\in(1;N))\ \chi_j=\frac{2\pi\cdot j}{Ly},(j\in(1;M)).$$

Graphically, depending on the parameter values *i* and *j* function $Q(x,y)$ shown in Figures 6-9.

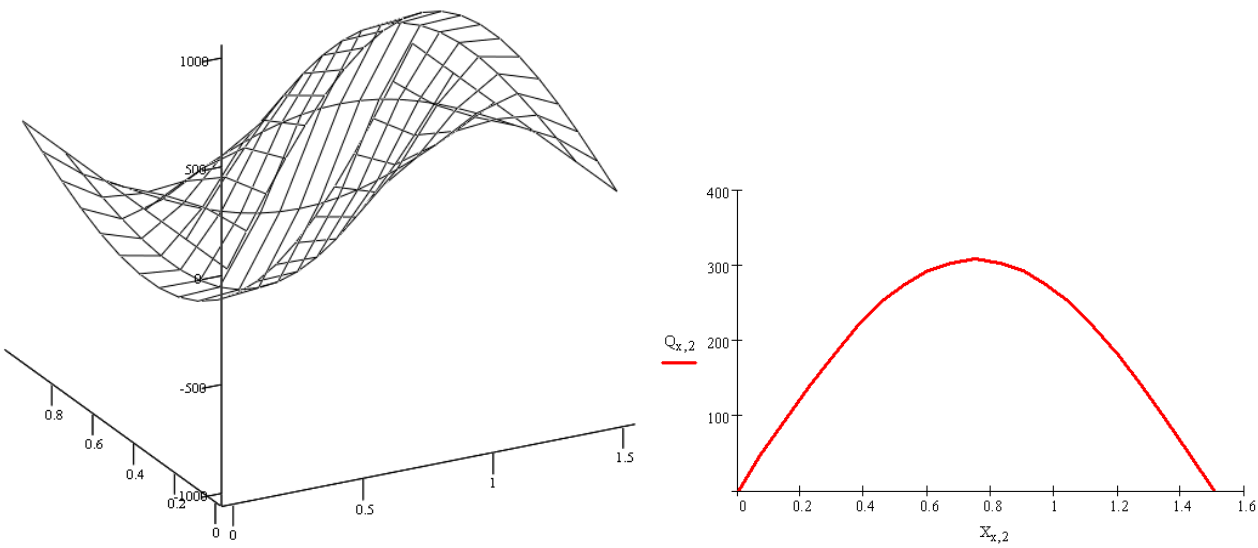


**Figure-6.** Graph of function $T(x,y)$ where $i=1,\ j=1$.

©2006-2021 Asian Research Publishing Network (ARPN). All rights reserved.


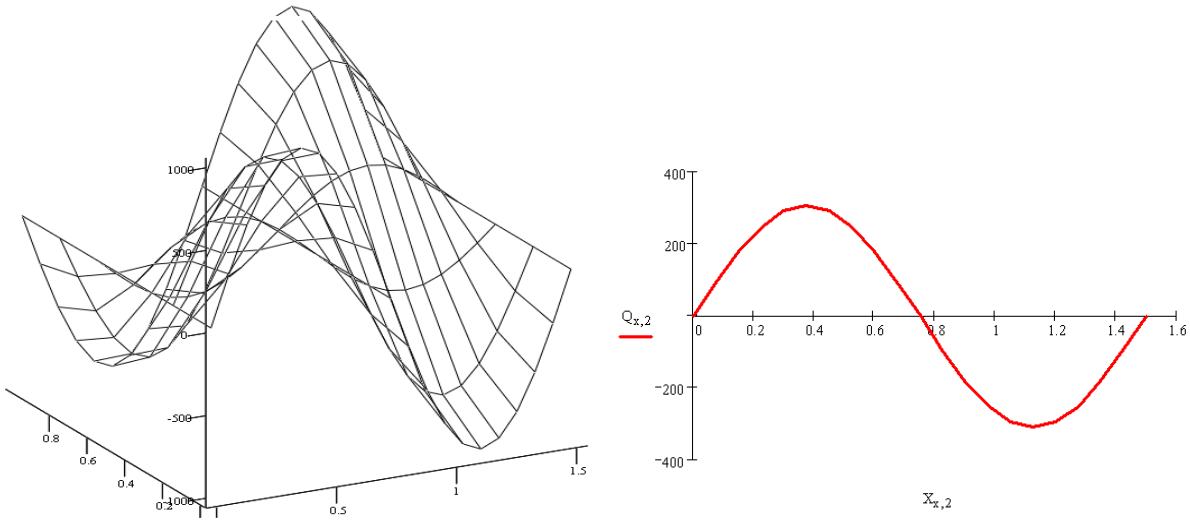


**Figure-7.** Graph of function $T(x, y)$ where $i = 2, j = 1$.

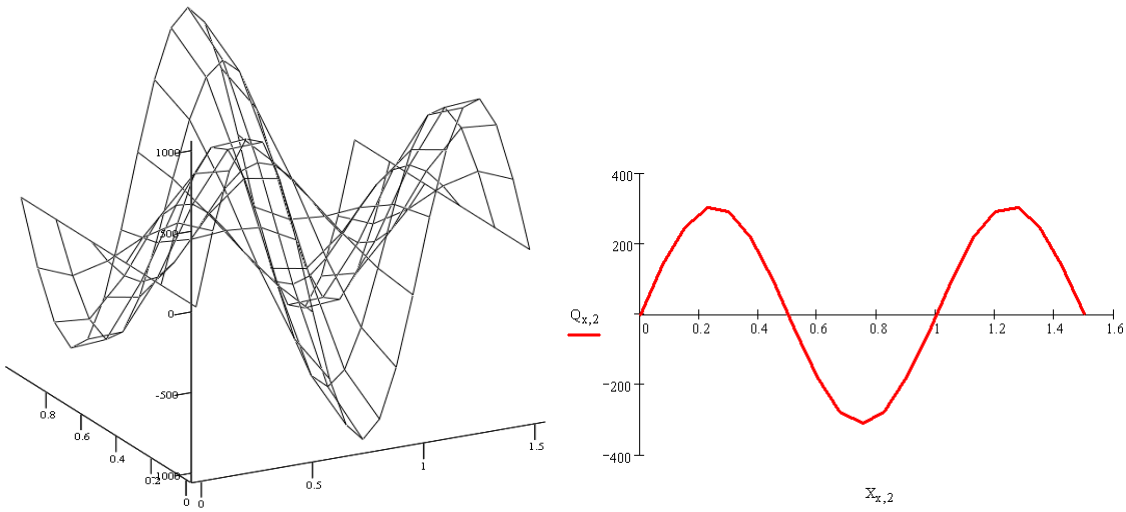


**Figure-8.** Graph of function $T(x, y)$ where $i = 3, j = 1$.

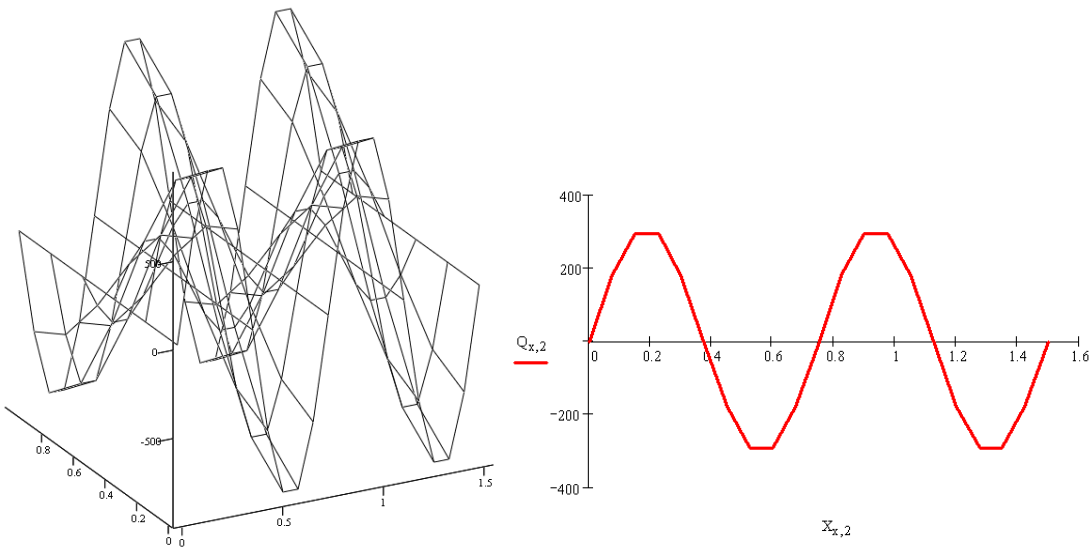


**Figure-9.** Graph of function $T(x, y)$ where $i = 3, j = 1$.

©2006-2021 Asian Research Publishing Network (ARPN). All rights reserved.


At the same time, at the input and output of the object, at a fixed point along the y coordinate, the graphs of the input functions were obtained $Q(x)$, exit $T(x)$, in steady state, and the schedule of the transient at a given point $T(\tau)$.

Next, using the obtained data, we will construct the frequency characteristics of the object under study. For this, we approximate the transfer functions of the object, for each mode of the input action as an aperiodic link with a pure delay:

$$W(G,p)=\frac{k(G)}{T_P(G)\cdot p+1}\cdot e^{-p\cdot\tau_P(G)},$$

where $k(G), T_P(G), \tau_P(G)$ - constants determined using transient graphs, linearization method, $p$ - Laplace operator, $G$ - generalized coordinate. System gain $k(G)$ is determined from the relation:

$$k(G)=\frac{T\max}{Q_{BX}},$$

where $T\max$ - steady-state value of the output function, $Q_{BX}$ - input action.

Let us determine the constants for the complex transfer coefficients for each mode of the input action. As the simulation results show, the system has the property of filtering spatial modes. Using the obtained transfer functions of the object, we construct the frequency characteristics of the open-loop system (Figures 10, 11).

Further, taking into account the obtained frequency characteristics of the control object, as well as the specified stability margins in modulus and phase, we will synthesize a distributed high-precision controller.

The synthesis of controllers for distributed objects (systems) of control with vector input action is the broadest area of synthesis of systems with distributed parameters. [7, 9, 11, 15].

As a rule, when studying an object, the input action on it is represented by a vector - functions (Fourier series in spatial coordinates), which are combinations of sines and cosines [9].

Issues of synthesis of controllers for control systems of distributed objects are reviewed in [7-11], while it was assumed that the system has one input and one output.

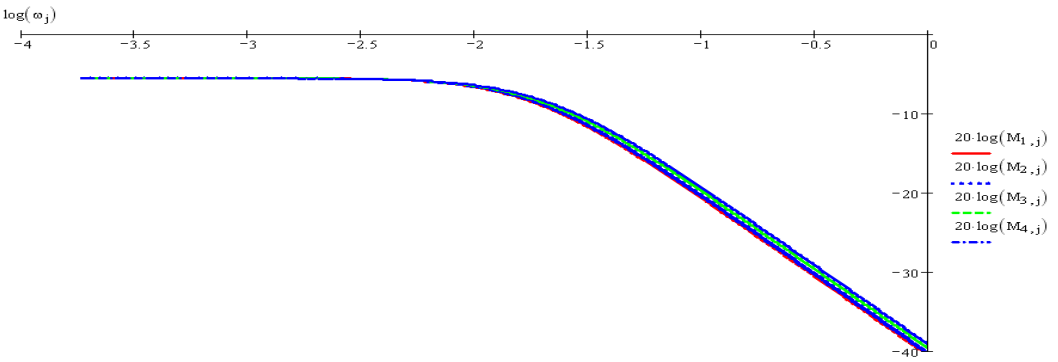


**Figure-10.** Object logarithmic frequency response.

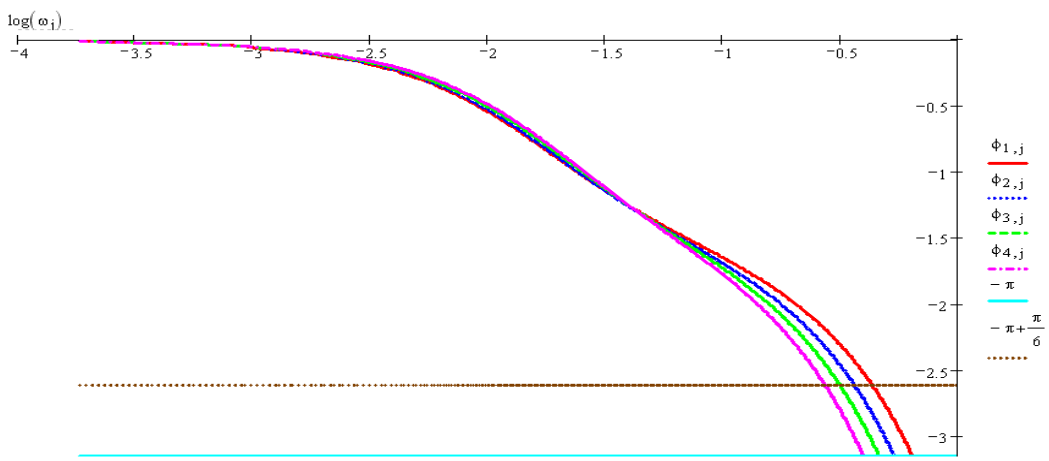


**Figure-11.** Object logarithmic phase-frequency response.

©2006-2021 Asian Research Publishing Network (ARPN). All rights reserved.


The results obtained in [7-11] can be used in the distributed objects control systems controllers synthesis which do not belong to the class of space-invariant, as well as in the synthesis of controllers for control systems with a vector input action.

Consider a graphical interpretation of the Nyquist criterion for assessing the stability of systems that do not belong to the class of spatially invariant, it should be noted that in [7-11], using a graphical interpretation of the Nyquist stability criterion, a methodology for the synthesis of controllers for distributed systems with a vector input action was developed.

This section provides a graphical interpretation of the Nyquist criterion for assessing the stability of systems that do not belong to the class of spatially invariant [7-11].

The amplitude and phase frequency characteristics of the hodographs of eigenvalues can be used to assess the stability of a closed system.

When constructing characteristics, we will assume that $|\lambda_1(0)| > |\lambda_2(0)| > |\lambda_3(0)| > \ldots$

$$L_i = 20 \cdot \lg|\lambda_i(j\omega)|, \qquad \varphi_i = arctg\left(\mathrm{Im}\lambda_i(j\omega) \big/ \mathrm{Re}\lambda_i(j\omega)\right),$$

( $i = \overline{1,\infty}$ ).

The interpretation of the Nyquist criterion, taking into account the constructed frequency characteristics, is as follows: let the transfer function of an open-loop system have no poles lying in the right half-plane. Then, for the stability of the closed-loop system, it is sufficient that the cut line of the module has no common points with the domain G.

Using the obtained interpretation of the Nyquist criterion, it is possible to determine the values of the input and output coefficients at which the closed-loop system will be stable and the stability margins of the hodographs of the eigenvalues in absolute value and in the phase of the open-loop system are not less than specified.

It should be noted that the determination of the hodographs location boundaries of the matrix eigenvalues under consideration can be carried out using the Gershgorin spectra.

## NUMERICAL EXAMPLE

To synthesize the coefficients of the space-amplification law, it is necessary to determine the desired gain of the controller. They are determined from the LAFC.

We obtain the real gains of the controller after synthesizing the parameters $E_1$, $n_1$ from the following system of equations:

$$\begin{cases} K_{\Pi}(G_1) = E_1 \cdot \left[\dfrac{n_1 - 1 + G_1}{n_1}\right] = 46.45833 \\ K_{\Pi}(G_6) = E_1 \cdot \left[\dfrac{n_1 - 1 + G_6}{n_1}\right] = 24.86275 \end{cases} \tag{31}$$

where $K_{\Pi}(G_1)$, $K_{\Pi}(G_6)$ – gain factors.

Dividing the first equation of system (31) by the second, we obtain an equation for finding $n_1$:

$$\left[\frac{E_1 \cdot \left[\dfrac{n_1 - 1 + G_1}{n_1}\right]}{E_1 \cdot \left[\dfrac{n_1 - 1 + G_6}{n_1}\right]}\right] = 1.868592, \tag{32}$$

$n_1 = -154.805227$ .

Then we transform the system of equations (31) to the form

$$\begin{cases} K(G_1) \cdot n_1 = E_1 \cdot n_1 - 1 + E_1 \cdot G_1 \\ K(G_6) \cdot n_1 = E_1 \cdot n_1 - 1 + E_1 \cdot G_6 \end{cases}, \tag{3.5}$$

Subtracting from the 1st equation the 2nd we obtain the equality for determining the parameter $E_1$:

$$(K(G_1) - K(G_6)) \cdot n_1 = E_1 \cdot (G_1 - G_6).$$

From here

$$E_1 = \frac{(K(G_1) - K(G_6)) \cdot n_1}{G_1 - G_6}.$$

Substituting the values, we get:

$$E_1 = 50.809159.$$

To check the calculations done, it is necessary to solve the equation:

$$K(G_i) = E_1 \cdot \left[\frac{n_1 - 1 + G_i}{n_1}\right]. \tag{33}$$

Substituting $E_1$, $G_i$ and $n_1$ into the equation, we get:

$$K(G_1) = E_1 \cdot \left[\frac{n_1 - 1 + G_1}{n_1}\right] = 46.45833,$$

$$K(G_2) = E_1 \cdot \left[\frac{n_1 - 1 + G_2}{n_1}\right] = 42.139214,$$

$$K(G_3) = E_1 \cdot \left[\frac{n_1 - 1 + G_3}{n_1}\right] = 34.940688,$$

$$K(G_4) = E_1 \cdot \left[\frac{n_1 - 1 + G_4}{n_1}\right] = 24.86275.$$

©2006-2021 Asian Research Publishing Network (ARPN). All rights reserved.


Due to the fact that $n_1$ cannot be negative, let's take it equal to one. Then the transfer function of the controller takes the form:

$$W(x, y, s) = 50,809159 \cdot \nabla \cdot 2, \quad (34)$$

where $\nabla$ - Laplacian.

As a result of calculations, the real values of the amplification factors of the space-amplifying link were obtained. The graphs of the desired and actual gains are shown in Figure-12.

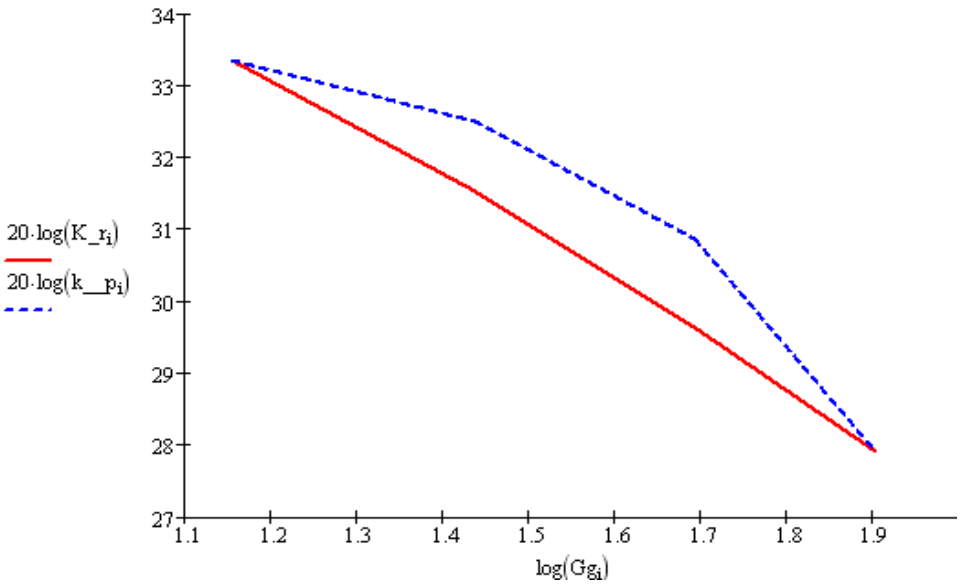


**Figure-12.** Dependency of the desired $20\lg(K_{ЖК}(G))$ and real $20\lg(K_P(G))$ regulator gains.

Next, we define the integrating and differentiating components of the distributed high-precision controller.

Parameters $E_1$, $n_1$ for the proportional component we take from [7-11], due to the fact that the phase shift introduced into the system by the PID controller is zero.

To define parameters $E_2$, $E_4$, $n_2$, $n_4$ it is necessary to solve the following system of equations:

$$\begin{cases} \lg(\omega(G_1)) = 0.5\lg\cdot\left[E_4\cdot\left[\dfrac{n_4-1+G_1}{n_4}\right]\right] - 0.5\lg\cdot\left[E_2\cdot\left[\dfrac{n_2-1+G_1}{n_2}\right]\right], \\ \lg(\omega(G_4)) = 0.5\lg\cdot\left[E_4\cdot\left[\dfrac{n_4-1+G_4}{n_4}\right]\right] - 0.5\lg\cdot\left[E_2\cdot\left[\dfrac{n_2-1+G_4}{n_2}\right]\right]. \end{cases} \quad (35)$$

Subtracting the first from the second equation, we get:

$$lg(\Delta\omega^2) = lg\left(\frac{n_4-1+G_4}{n_4-1+G_1}\right) - lg\left(\frac{n_2-1+G_4}{n_2-1+G_1}\right) \quad (36)$$

We get that $\omega(G_1) = 0.431777$, $\omega(G_4) = 0.271107$.

Then we define $\Delta\omega^2$:

$$\Delta\omega^2 = \frac{(\omega(G_4))^2}{(\omega(G_1))^2} = 0.394239 .$$

Because $\Delta\omega^2 > 0$, than $n_2$ we take equal to $\infty$ [6-10]. Substituting $n_2$ into equation (36) and transforming, we obtain an equation for determining $n_4$:

$$n_4 = \frac{(\Delta\omega^2 - 1 + G_4 - \Delta\omega^2 \cdot G_1)}{\Delta\omega^2 - 1} .$$

As a result, we get that $n_4 = 29.565954$ .

The constraint equation can be represented as:

$$\Delta(G_1) = \lg \varpi_1 - \lg \varpi_2 , \quad (37)$$

$$\lg \varpi_1 = \lg\left[\frac{1}{K_2(G_1)}\right], \ \lg \varpi_2 = \lg[K_4(G_1)],$$

©2006-2021 Asian Research Publishing Network (ARPN). All rights reserved.


$$\Delta(G_1) = \lg\left[\frac{1}{K_2(G_1)}\right] - \lg[K_4(G_1)].$$

In our case, using experimental data, the value $\Delta(G_1)$ equals to 0,5. From the resulting system of equations (37), we find $E_2$ and $E_4$:

$$\begin{cases} \lg(\omega(G_1)) = 0.5\lg\cdot\left[E_4\cdot\left[\frac{n_4-1+G_1}{n_4}\right]\right] - 0.5\lg\cdot\left[E_2\cdot\left[\frac{n_2-1+G_1}{n_2}\right]\right] \\ \Delta(G_1) = \lg\left[\frac{1}{E_2\cdot\left[\frac{n_2-1+G_1}{n_2}\right]}\right] - \lg\left[E_4\cdot\left[\frac{n_4-1+G_1}{n_4}\right]\right]. \end{cases} \quad (38)$$

Having solved the resulting system of equations, we obtain:
$E_4 = 0{,}167643.$

To find $E_2$ we multiply the equations of system (37) with each other, after the transformation, we obtain: $E_2 = 1{,}302387$ .

Thus, the transfer function of the synthesized controller will take the following form:

$$W(x, y, s) = 50{,}809159217\cdot\nabla\cdot 2 - 1{,}30238684231519\cdot s + 0{,}16764262\,(0{,}966177 - 0{,}033823\cdot\nabla\cdot 2)\,\frac{1}{s}. \quad (39)$$

To construct the integral branch of the graph, we solve the system of equations:

$$\begin{cases} \lg[\omega_H(G_i)] = \lg[K_4(G_i)], \\ \lg[\omega_H(G_i)] = \lg\left[E_4\cdot\left[\left(\frac{n_4-1}{n_4}\right)+\left(\frac{1}{n_4}\right)\cdot G_i\right]\right] \\ \lg[\omega_H(G_1)] = \lg\left[E_4\cdot\left[\left(\frac{n_4-1}{n_4}\right)+\left(\frac{1}{n_4}\right)\cdot G_1\right]\right] = -0.61474, \\ \lg[\omega_H(G_2)] = \lg\left[E_4\cdot\left[\left(\frac{n_4-1}{n_4}\right)+\left(\frac{1}{n_4}\right)\cdot G_2\right]\right] = -0.498363, \\ \lg[\omega_H(G_3)] = \lg\left[E_4\cdot\left[\left(\frac{n_4-1}{n_4}\right)+\left(\frac{1}{n_4}\right)\cdot G_3\right]\right] = -0.354792, \\ \lg[\omega_H(G_4)] = \lg\left[E_4\cdot\left[\left(\frac{n_4-1}{n_4}\right)+\left(\frac{1}{n_4}\right)\cdot G_4\right]\right] = -0.2105. \end{cases} \quad (40)$$

To construct the differential branch of the graph, we solve the system of equations:

$$\begin{cases} \lg[\omega_Д(G_i)] = \lg[K_2(G_i)], \\ \lg[\omega_Д(G_i)] = \lg\left[\frac{1}{E_2\cdot\left[\left(\frac{n_2-1}{n_2}\right)+\left(\frac{1}{n_2}\right)\cdot G_i\right]}\right], \\ \lg[\omega_Д(G_i)] = \lg\left[\frac{1}{E_2\cdot\left[\left(\frac{\infty-1}{\infty}\right)+\left(\frac{1}{\infty}\right)\cdot G_i\right]}\right] = -0.11474. \end{cases} \quad (41)$$

When checking the performed transformations and the calculated parameters, it was obtained:

$$\left|\lg[\omega_Д(G_i)] - \lg[\omega_H(G_i)]\right| = \left|-0{,}61474 + 0{,}11474\right| = 0{,}5.$$

Which confirms the correctness of the calculations.

Based on the data obtained, we build graphs of the amplitude frequency characteristics of the control object and the controller (Figures 13-16).

Next, we analyze the closed-loop control system. Research will be carried out on a numerical model.

## CLOSED-LOOP CONTROL SYSTEM ANALYSIS

As a result of numerical simulation on a computer of a closed automatic control system in the air gaps of the heating chamber for heat treatment, graphs of transient processes were obtained.

©2006-2021 Asian Research Publishing Network (ARPN). All rights reserved.


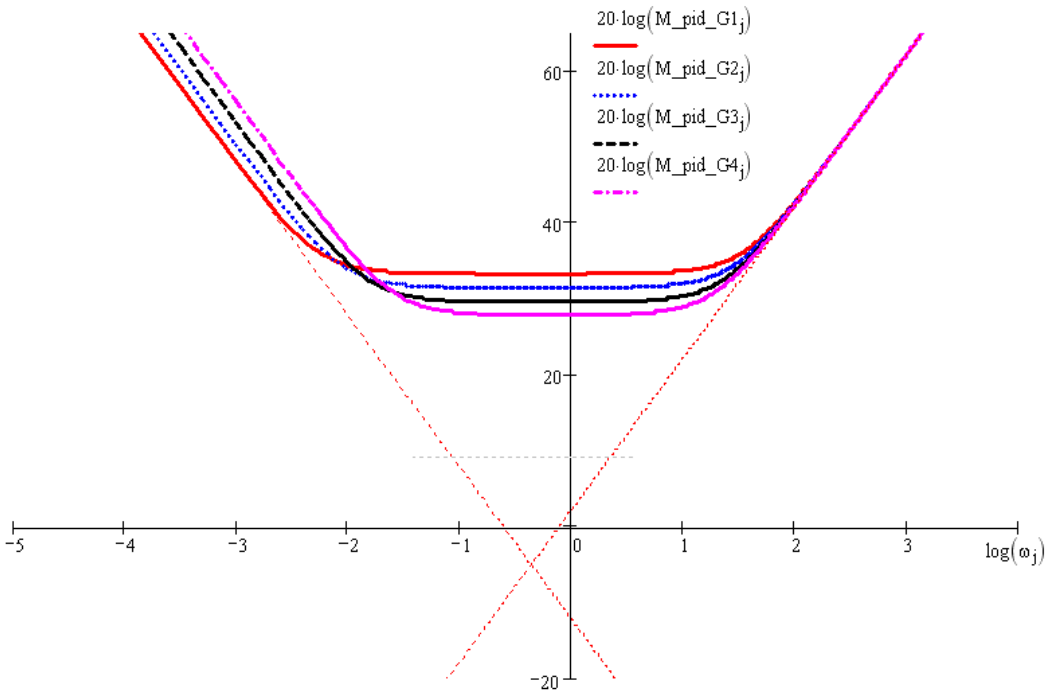


**Figure-13.** LAFC of distributed high-precision regulator.

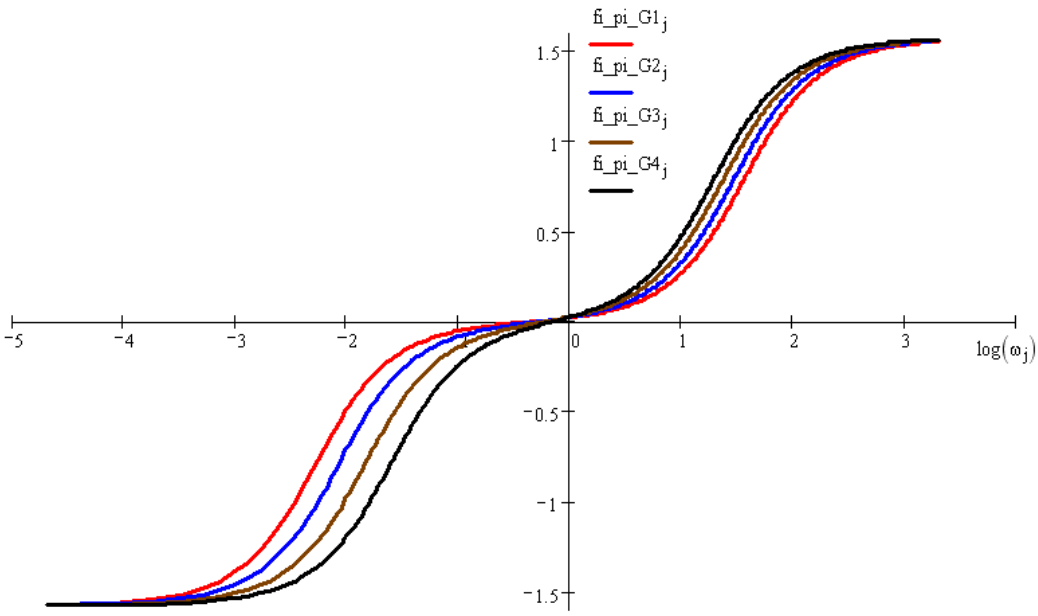


**Figure-14.** LPFC of the distributed high-precision regulator.

©2006-2021 Asian Research Publishing Network (ARPN). All rights reserved.


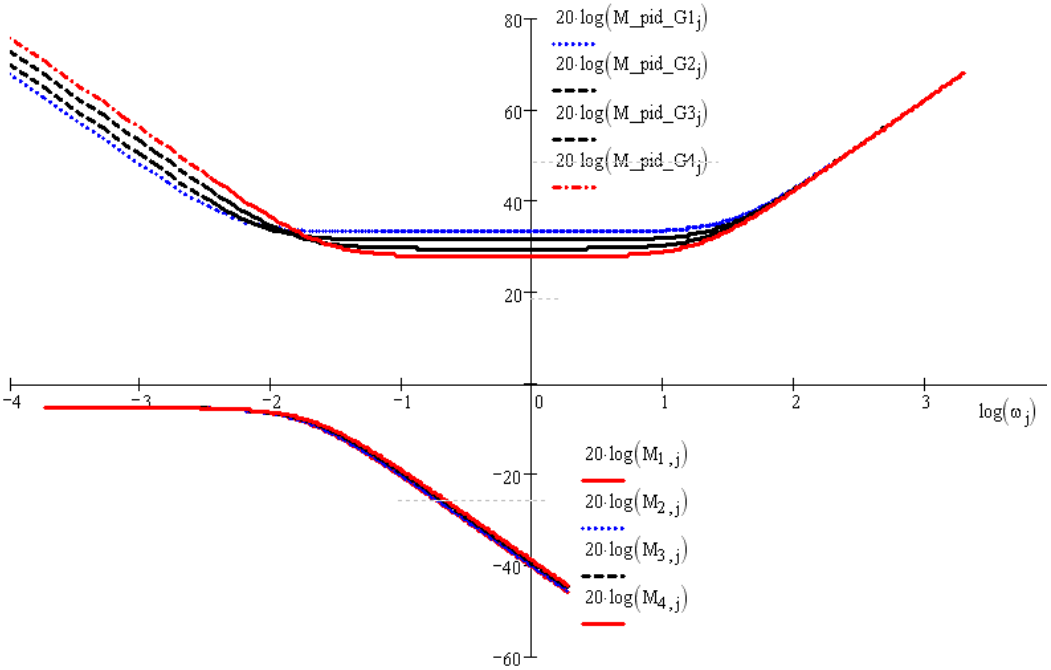


**Figure-15.** LAFC of distributed high-precision regulator and object.

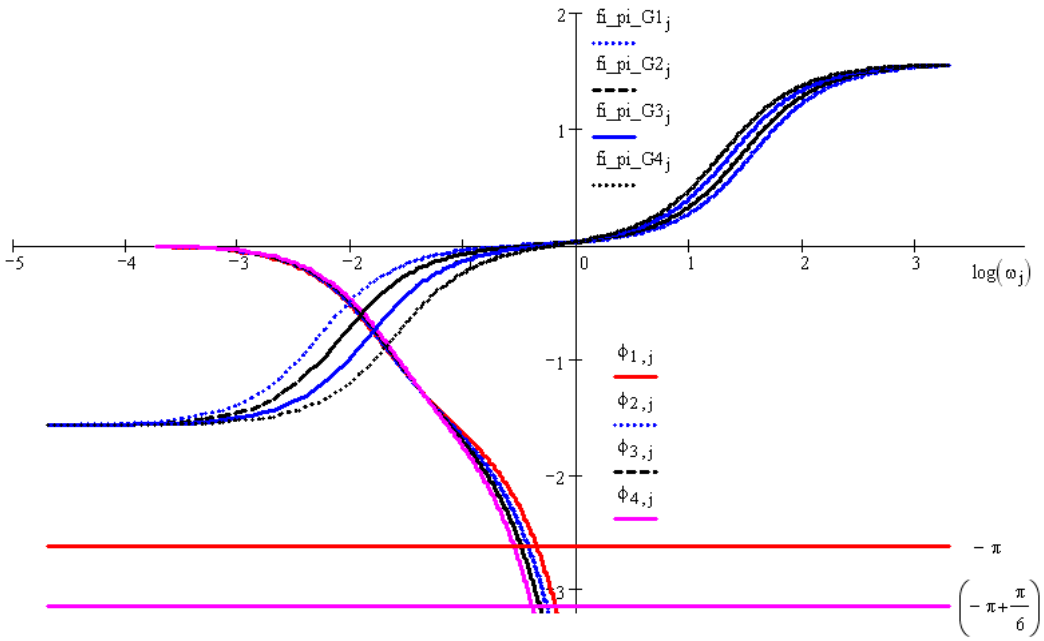


**Figure-16.** LPFC distributed: high-precision regulator and object.

When the level of the control action was limited by the mark $2000^0 C$ and the reference action equal $600^0 C$, the graphs of transient processes at the output of the object were obtained, shown in Figure-17.

©2006-2021 Asian Research Publishing Network (ARPN). All rights reserved.


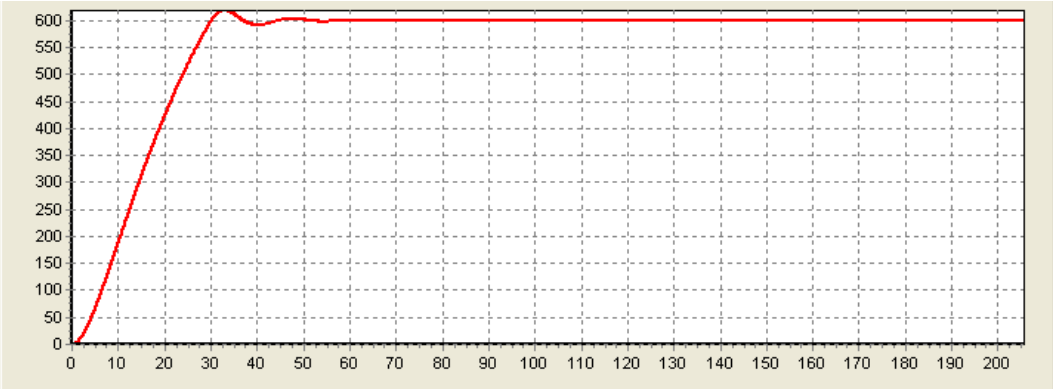


**Figure-17.** Graph of the transient process of a closed ACS at a point [3, 2, NZ4-1].

With the limitation of the control action level by the mark $1400^0C$ and the reference action equal $600^0C$, the graphs of transient processes at the output of the object were obtained, shown in Figure-18.

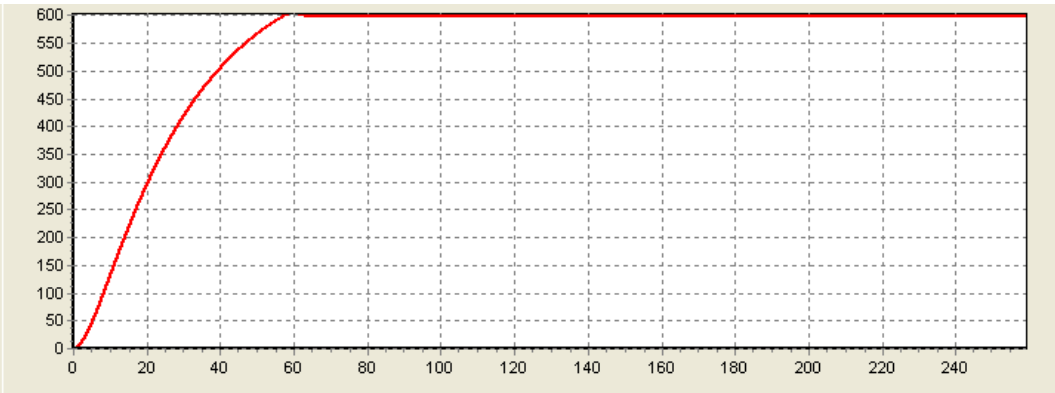


**Figure-18.** Graph of the transient process of a closed ACS at a point [3, 2, NZ4-1].

With the limitation of the control action level by the mark $1200^0C$ and the reference action equal $600^0C$, the graphs of the transient processes at the output of the object were obtained, shown in Figure-19.

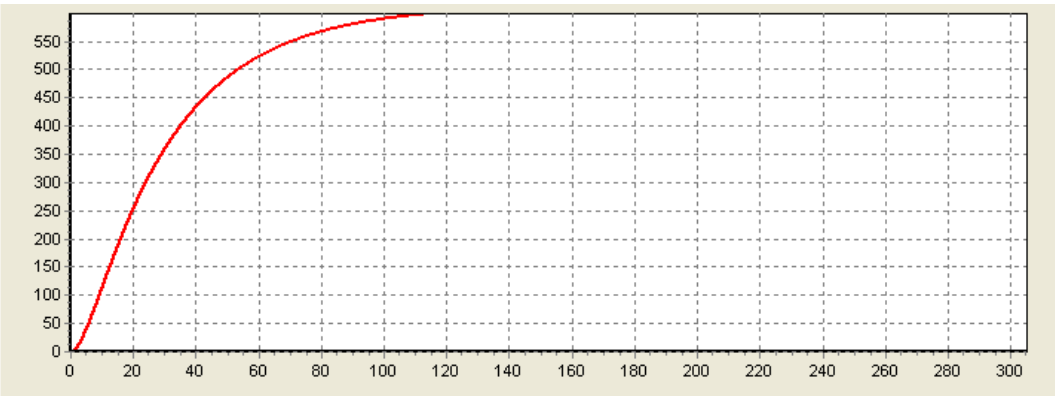


**Figure-19.** Graph of the transient process of a closed ACS at a point [3, 2, NZ4-1].

As the simulation results show, the control system is stable, and the control error tends to zero.

## CONCLUSIONS

The analysis of the closed-loop automatic control system was carried out for several cases of limiting the control action level by marks: $1200^0C$; $1400^0C$; $2000^0C$. In this case, the exit function stabilized at the mark $600^0C$ with an error of about $1^0C$. In this case, the regulation time decreases with an increase in the limiting value of the control signal level.

It is desirable to implement the distributed regulator developed in this study using programmable

©2006-2021 Asian Research Publishing Network (ARPN). All rights reserved.


microcontrollers and control output modules, since it will be necessary to implement a partial derivative with respect to spatial coordinates and work with different values of the time constants of the integrating elements, which are rather problematic to implement using analog equipment, due to the large dimensions of non-polar electrolytic capacities. It is also worth noting that the number of control actions of such systems can include space-time controls described by functions of several arguments - time and spatial coordinates. Then such systems require additional revision. For example, in the production of high-strength, chemically resistant glass, it is necessary to take into account the effect of the catalyst on the generated thermal field. However, the development of such control systems requires the creation of a new apparatus based on mathematical tools that are non-traditional for the classical control theory. What will be the subject of further research and development.

**ACKNOWLEDGEMENTS**

We should note that persons without whom these studies could not have been carried out. The first is Pershin Ivan Mitrofanovich (Doctor of Technical Dciences, Professor, actual member of the Academy of Natural Sciences, Honored Worker of Higher Professional Education of the Russian Federation), Kolesnikov Anatoly Arkadievich (Honored Worker of Science and Technology of the Russian Federation, Doctor of Technical Sciences, Professor, member of the Academy of Sciences and the Academy of electrical-technical sciences and Motion Control, Corresponding Member of the Russian Academy of Natural Sciences, Soros Professor (four) in the exact sciences field), and Chernyshev Alexander Borisovich (Doctor of Technical Sciences, Professor) who laid the foundation for the synthesis of distributed controllers on the basis of the Green's function.

**REFERENCES**

[1] Kogan V.E. 2016. Glassy foams of inorganic and organic nature and the prospects for cleaning the environment from pollution by oil and oil products. Journal of Mining Institute, [S.l.], 218: 331. ISSN 2541-9404. Available at: <http://pmi.spmi.ru/index.php/pmi/article/view/23>. Access date: 19 March 2020.

[2] Kogan V.E. 2017. Chemistry as a basis for solving environmental problems / V.E. Kogan; T.S. Shakhparonov. Journal of Mining Institute, [S.l.], 224: 223. ISSN 2541-9404. Available at: <http://pmi.spmi.ru/index.php/pmi/article/view/5240> . Access date: 19 March 2020.doi: http: //dx.doi.org/10.18454/pmi.2017.2.223

[3] Asadulagi M.M. Stochastic control system of hydrodynamic processes in aquifers/ M.M. Asadulagi, D.A. Pervukhin. Innovation-Based Development of the Mineral Resources Sector: Challenges and Prospects - 11th conference of the Russian-German Raw Materials, 2018 c. 175-185.

[4] Ilyushin A.N., Development of Information Measuring Complex of Distributed Pulse Control System / A. N. Ilyushin, D. A. Kovalev, P. M. Afanasev. 2019 International Multi-Conference on Industrial Engineering and Modern Technologies (FarEastCon), Vladivostok, Russia, 2019, pp. 1-5. DOI: 10.1109/FarEastCon.2019.8934173

[5] Ilyushin A.N. 2019. Design of Automated Control System Supporting Temperature Field in / A.N. Ilyushin, I.D. Shilkina, P.M. Afanasev. International Multi-Conference on Industrial Engineering and Modern Technologies, FarEastCon 2019. Vladivostok, Russia, pp. 1-4. DOI: 10.1109/FarEastCon.2019.8934041

[6] Kazanin O.I. 2018. Numerical study of the air-gas dynamic processes when working out the Mosshny seam with longwall faces / O.I. Kazanin, A.A. Sidorenko, Y.G. Sirenko. ARPN Journal of Engineering and Applied Sciences. 13(4): 1534-1538.

[7] Kukharova T.V. 2018, 2019. Conditions of Application of Distributed Systems Synthesis Methods to Multidimensional Object/ T.V. Kukharova, I.M. Pershin. 2018 International Multi-Conference on Industrial Engineering and Modern Technologies, FarEastCon, № 8602749 DOI: 10.1109/FarEastCon.2018.8602749.

[8] Kukharova T.V. 2018, 2019. Observation and Prediction Systems Modeling for Human Mental State/ T.V. Kukharova, V.A. Utkin, I.V. Boev. 2018 International Multi-Conference on Industrial Engineering and Modern Technologies, FarEastCon, № 8602831 DOI: 10.1109/FarEastCon.2018.8602831.

[9] Martirosyan A.V. 2019. Application of Fourier series in Distributed Control Systems Simulation [Text] / A.V. Martirosyan, K.V. Martirosyan, A.B. Chernyshev. 2019 IEEE Conference of Russian Young Researchers in Electrical and Electronic Engineering (EIConRus) (January 28-31). - St. Petersburg, pp. 609-613. DOI: 10.1109/EIConRus.2019.8656865

[10] Martirosyan A.V. 2016. Methods of distributed systems structured modeling [Text] / A.V. Martirosyan, K.V. Martirosyan, A.B. Chernyshev.

©2006-2021 Asian Research Publishing Network (ARPN). All rights reserved.


2016 IEEE NW Russia Young Researchers in Electrical and Electronic Engineering Conference (February 2-3). - St. Petersburg, pp. 283-289. DOI: 10.1109/EIConRusNW.2016.7448175

[11] Martirosyan A.V. 2016. Quality improvement information technology for mineral water field's control [Text] / A.V. Martirosyan, K.V. Martirosyan // 2016 IEEE Conference on Quality Management, Transport and Information Security, Information Technologies (October 4-11). - Nalchik, pp. 147-151. DOI: 10.1109/ITMQIS.2016.7751925

[12] Sidorenko A.A. 2018. Influence of face advance rate on geomechanical and gas-dynamic processes in longwalls in gassy mines / A.A. Sidorenko, Yu.G. Sirenko, S.A. Sidorenko. Eurasian Mining, 1, pp. 3-8. DOI: 10.17580/em.2018.01.01.

[13] Schipachev A. 2018. Optimum Conditionsof Turning and Surface Plastic Defomation DeterminationTaking into Account Technological Heredity. Journal of Physics: Conference Series, 1118(1): 012036 DOI: 10.1088/1742-6596/1118/1/012036

[14] Shipachev A.M. 2018. Phenomenon of low-alloy steel parametrization transformation at cyclic loading in low-cyclic area / A.M. Shipachev, M.N. Nazarova. IOP Conference Series: Earth and Environmental Science, 87(9): 092017 DOI: 10.1088/1755-1315/87/9/092017

[15] Verzhbitskiy K., Samigullin G., Schipachev A. 2018. Increasing service life of chuck unit of tank during cyclic loading / K. Verzhbitskiy, G.Samigullin, A. Schipachev. Journal of Physics: Conference Series, 1118(1): 012040 DOI: 10.1088/1742-6596/1118/1/012040